Electrode Materials

DOI: 10.1002/ange.200501663

Synthesis of Nanowire and Mesoporous Low-Temperature $LiCoO_2$ by a Post-Templating Reaction**

*Feng Jiao, Kuthanapillil Mani Shaju, and Peter G. Bruce**

The synthesis of transition-metal oxides with controlled nanostructures, such as mesoporous solids, nanotubes, or nanowires, is an important task because such nanostructuring may have a profound influence on the properties of these materials.[1–3] This includes nanostructured materials for energy conversion and storage.[4] Soft templating routes have been used to synthesize mesoporous transition-metal compounds, for example, Nb_2O_5, TiO_2, MnO_x, and Fe_2O_3; however, the materials often have poorly crystallized walls and are thermally unstable, which limits their applications.[3,5]

The introduction of hard templating methods represents a significant step forward in the synthesis of mesoporous solids.[6,7] Solution-based precursors of the desired phase may be loaded within the pores of a mesoporous silica, and, after firing, the hard silica template may be removed to yield a mesoporous compound with highly crystalline walls and good thermal stability. Such nanocasting approaches have been used to form several transition-metal oxides, for example, Cr_2O_3, Fe_2O_3, MnO_x, CeO_2, Co_3O_4, and WO_3.[8–11] The nanocasting method is, however, limited to the use of precursors that do not react with the hard template and to compounds that may be prepared within the temperature range over which the silica template is stable. The former problem renders it difficult to synthesize mesoporous oxides that contain alkali metals. However, the synthesis of nanostructured oxides containing lithium is essential if such materials are to be used as positive electrodes in rechargeable lithium batteries, as the positive electrode is the only source of Li in the cells (the negative electrode is graphite). Mesoporous materials are attractive for electrodes because the controlled and regular porosity permits intimate flooding of the electrolyte within the particles. Hard-templated materials permit the formation of crystalline walls, which can be important in promoting Li intercalation.

Herein, we describe the synthesis of nanowire and mesoporous low-temperature $LiCoO_2$ (LT-$LiCoO_2$), a Li intercalation compound, by the hard template route. The synthesis involves, first, preparation of mesoporous or nanowire Co_3O_4, then, after template removal, reaction of Co_3O_4 with a lithium source whilst retaining the nanostructured morphology. Hence, the lithium-containing compounds may be prepared by avoiding reaction between the lithium precursor and the silica template, which would occur if the compounds were prepared directly. The formation of large (≈100 nm) nanowire arrays of high-temperature $LiCoO_2$ within an anodic aluminum oxide membrane has been reported, however, the template was only partially removed.[12]

Two mesoporous silica compounds, SBA-15 and KIT-6, were used as hard templates.[7,13] The former contains parallel cylindrical pores arranged with hexagonal symmetry (space group *P6mm*). The latter has a three-dimensional cubic arrangement of pores (space group *Ia3d*). Such pore structures yield nanowire and mesoporous morphologies, respectively. The hard templates were impregnated with a solution of cobalt nitrate in ethanol, calcined at 300 °C, impregnated again to maximize pore filling, and heated at 500 °C, then the silica templates were removed with aqueous HF. Analysis by energy dispersive X-ray spectroscopy (EDX) and inductively coupled plasma demonstrated that all the silica had been removed. Flame emission and atomic absorption spectrometry confirmed that the Li-to-Co mole ratios for nanowire and mesoporous LT-$LiCoO_2$ samples were 0.95:1.

The nanowire structure of Co_3O_4 arising from SBA-15 is shown in Figure 1 A and B. SBA-15 comprises short bridges between the cylindrical pores and these serve to organize the wires into parallel bundles.[9] Co_3O_4 formed from KIT-6 has a cubic nanostructure replicating the pore structure of the template (Figure 1 C and D). Mesoporous Co_3O_4, with *Ia3d* symmetry, was prepared for the first time very recently.[11] It

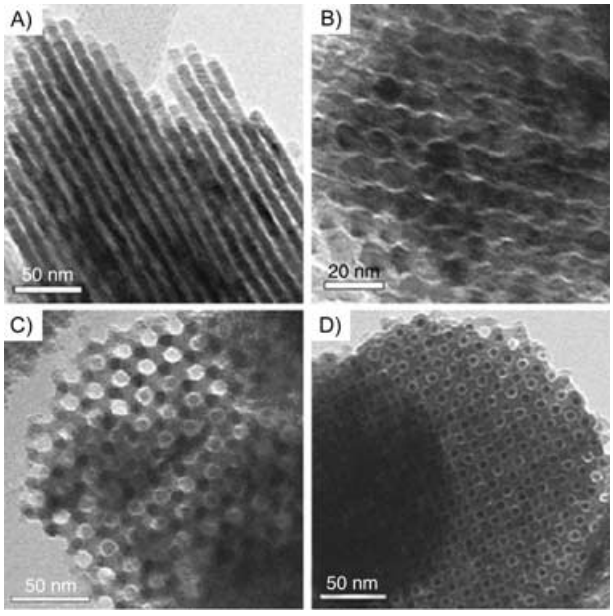

Figure 1. TEM images of Co_3O_4 nanowires A) perpendicular and B) parallel to the wire axis. TEM images of mesoporous Co_3O_4 along the C) [111] and D) [100] directions.

[*] F. Jiao, Dr. K. M. Shaju, Prof. P. G. Bruce
School of Chemistry
University of St. Andrews
The Purdie Building, North Haugh, St Andrews KY16 9ST (UK)
Fax: (+44) 1334-463808
E-mail: p.g.bruce@st-and.ac.uk

[**] P.G.B. is indebted to the EPSRC, the EU, and The Royal Society for financial support.

Supporting information for this article is available on the WWW under http://www.angewandte.org or from the author.

InterScience
© 2005 Wiley-VCH Verlag GmbH & Co. KGaA, Weinheim

was found necessary to functionalize the pores by attaching vinyl groups to provide superior coordination of Co ions and hence high loadings. As demonstrated here, this is not essential.[10]

Nanowire and mesoporous LT-$LiCoO_2$ samples were prepared by reacting the respective nanostructured Co_3O_4 materials with LiOH at 400 °C for 1 h. $LiCoO_2$ synthesized at around 800 °C exhibits a layered α-$NaFeO_2$ structure, whereas synthesis at lower temperatures yields LT-$LiCoO_2$ composed predominantly of a spinel structure that contains additional lithium, $Li_2Co_2O_4$.[14,15] LT-$LiCoO_2$ was anticipated from the temperature at which the synthesis was performed, and this was verified by wide-angle powder X-ray diffraction (PXRD, Figure 2A). Although the diffraction data for high-temperature and low-temperature materials are similar, it is evident, especially on examining the insets in Figure 2A, that the material synthesized here is LT-$LiCoO_2$. The use of temperatures that are sufficiently high to promote the formation of HT-$LiCoO_2$ resulted in a loss of the nanostructure.

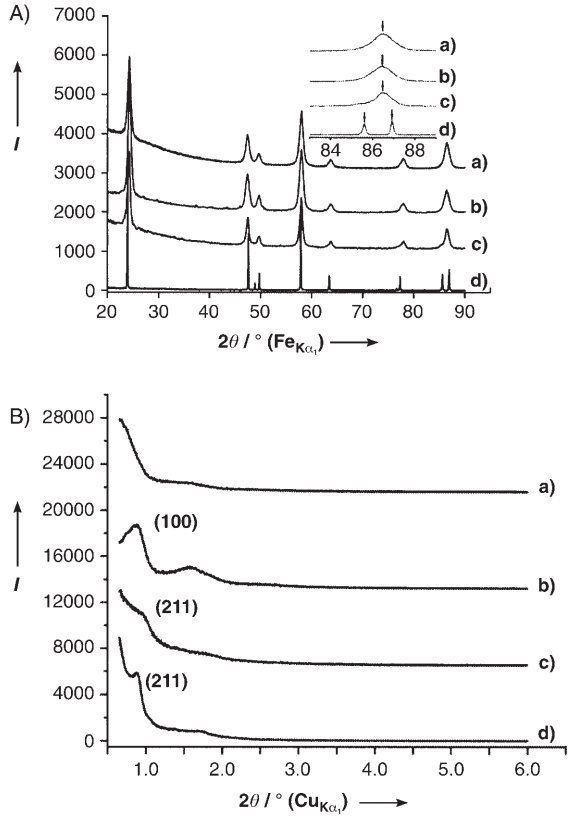

Figure 2. A) Wide-angle PXRD patterns: a) LT-$LiCoO_2$ nanowires; b) mesoporous LT-$LiCoO_2$; c) bulk LT-$LiCoO_2$; d) high-temperature $LiCoO_2$. The inset shows the expanded scale from 83–89°. B) Low-angle PXRD patterns: a) LT-$LiCoO_2$ nanowires; b) Co_3O_4 nanowires; c) mesoporous LT-$LiCoO_2$; d) mesoporous Co_3O_4.

The nanowire morphology of LT-$LiCoO_2$ prepared from SBA-15 is shown in Figure 3A–C. This morphology dominates throughout the material. Although the wires are continuous, close inspection of high-resolution transmission electron microscopy (HR-TEM) data (Figure 3C) indicate

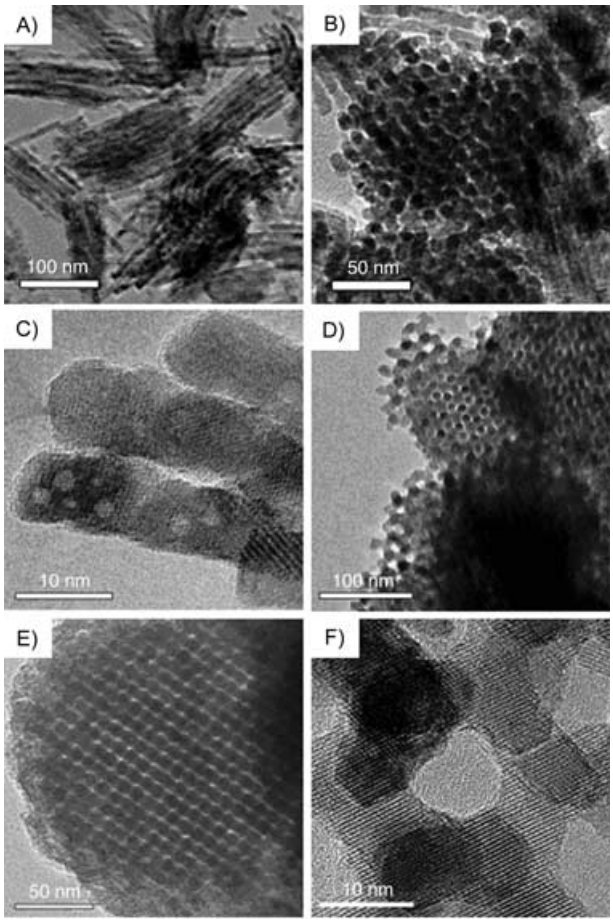

Figure 3. TEM images of LT-$LiCoO_2$ nanowires A) perpendicular and B) parallel to the wire axis, and C) high-resolution image of LT-$LiCoO_2$ nanowires. TEM images of mesoporous LT-$LiCoO_2$ along the E) [111] and F) [531] directions, and G) high-resolution image of mesoporous LT-$LiCoO_2$.

that they are composed of domains that are not structurally coherent. This is different from the single-crystal-like nature of the Co_3O_4 nanowires. However, importantly, the nanowire morphology of the Co_3O_4 material has been maintained. By TEM analysis, the diameter of LT-$LiCoO_2$ wires is measured as approximately 10 nm, only slightly larger than the value of 9.5 nm for Co_3O_4. Turning to mesoporous LT-$LiCoO_2$ formed from KIT-6, TEM data for this material are shown in Figure 3D–F. It is clear that the cubic mesoporous morphology of Co_3O_4 is maintained; the morphology extends throughout the sample. The wall thickness of mesoporous LT-$LiCoO_2$ observed in the [111] direction is estimated from the TEM data (Figure 3F) to be approximately 8.0 nm, which is consistent with that for Co_3O_4 (7.8 nm). In contrast to nanowire LT-$LiCoO_2$, it is interesting that mesoporous LT-$LiCoO_2$ maintains a single-crystal-like structure; the HR-TEM image (Figure 3F) indicates that the lattice fringes for LT-$LiCoO_2$ run in the same direction throughout the particle. Further studies will be required to understand the mechanism by which the single-crystal structure is maintained during reaction with LiOH.

 © 2005 Wiley-VCH Verlag GmbH & Co. KGaA, Weinheim

A comparison of Figures 1 and 3 reveals that the LT-$LiCoO_2$ nanowires are less ordered than the corresponding Co_3O_4 nanowires. The loss of order between the wires in LT-$LiCoO_2$ may be a result of the breaking up of narrow bridges on reaction with LiOH. Despite this, a lattice parameter a_0 of 108 Å may be estimated for the hexagonal (*P6mm*) mesostructure. This is in reasonable agreement with the value of 117 Å calculated from the low-angle PXRD pattern of the Co_3O_4 nanowires. The low-angle PXRD pattern of nanowire LT-$LiCoO_2$ (Figure 2B, line a) does not show a well-defined peak in the range 0.6–1.0 degrees because the nanowire bundles are insufficiently well ordered (Figure 3A). In the case of LT-$LiCoO_2$ formed from KIT-6, a lattice parameter, a_0 of 226 Å may be extracted for the cubic structure from the TEM data. This value is similar to the lattice parameter of 235 Å calculated from the first peak in the low-angle PXRD pattern of mesoporous LT-$LiCoO_2$ (Figure 2B, line c). This value is a little smaller than the parameter a_0 for mesoporous Co_3O_4 (241 Å) calculated from Figure 2B, line d, and is due to pore shrinkage accompanying the solid-state reaction.

N_2 adsorption/desorption isotherms (Figure 4A, B) for both forms of nanostructured LT-$LiCoO_2$ show type IV

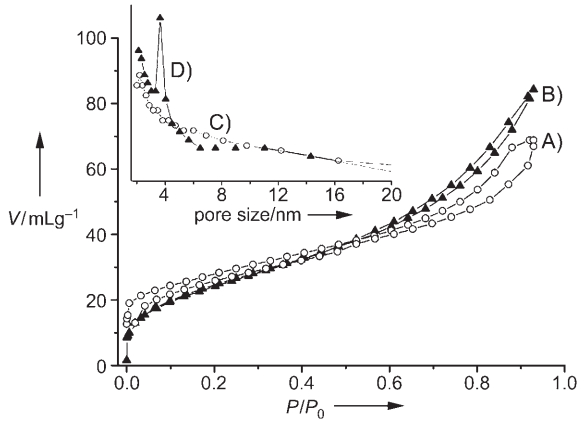

Figure 4. Nitrogen adsorption/desorption isotherms for A) nanowire and B) mesoporous LT-$LiCoO_2$. The inset shows the pore size distributions for C) nanowire and D) mesoporous LT-$LiCoO_2$.

isotherms with an H_1 hysteresis loop, which confirms the mesoporosity. The specific surface areas of nanowire and mesoporous LT-$LiCoO_2$ estimated from the Brunauer–Emmett–Teller (BET) method are 70 $m^2 g^{-1}$ and 92 $m^2 g^{-1}$, respectively. In the case of the LT-$LiCoO_2$ nanowires, the size of the pores between the wires exhibits a wide distribution (Figure 4C), indicating a disordered pore structure, which is consistent with the absence of a low-angle PXRD peak (Figure 2B, line a) and with the TEM images (Figure 3A, B); the more-ordered Co_3O_4 nanowires show a narrow distribution around 3.8 nm (see Supporting Information). In the case of mesoporous LT-$LiCoO_2$, the pore size distribution (Figure 4D) is narrow with a peak at 3.67 nm, which is close to the value for mesoporous Co_3O_4 (3.8 nm; see Supporting Information).

The present communication concentrates on the synthesis of LT-$LiCoO_2$ with different nanoarchitectures. The electrochemical behavior of these Li intercalation materials and their comparison with normal LT-$LiCoO_2$ will be described in a subsequent paper; however, some preliminary data are presented here. The surface area of the normal LT-$LiCoO_2$, prepared by a solid-state reaction between $CoCO_3$ and Li_2CO_3 at 400 °C, was 42 $m^2 g^{-1}$. The cells were first charged to remove lithium from the electrodes. Figure 5 reports the

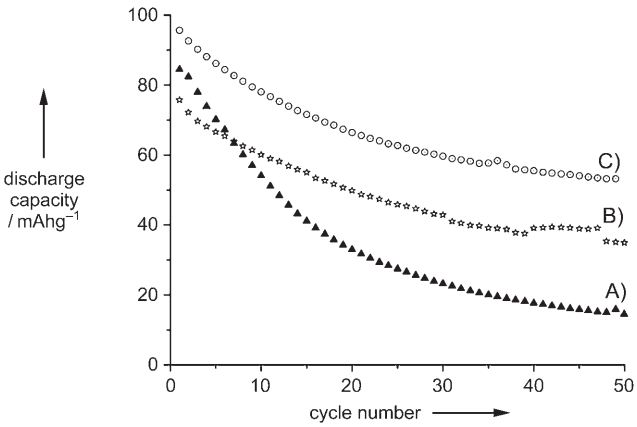

Figure 5. Discharge capacities for A) normal (▲), B) nanowire (*), and C) mesoporous (⊙) forms of LT-$LiCoO_2$.

discharge capacity for the first and subsequent cycles, for which cycling was carried out at a constant rate of 30 mA g^{-1} between potential limits of 3.0 V and 4.2 V. The first discharge capacity for mesoporous LT-$LiCoO_2$ is some 20 mA h g^{-1} higher than that for the equivalent nanowire material. The initial discharge capacity of normal LT-$LiCoO_2$ lies between the two nanostructured materials. The fade of discharge capacity on cycling is the same for both nanostructured forms of LT-$LiCoO_2$, however, the fade is markedly less than that of normal LT-$LiCoO_2$. The capacity of the nanostructured materials decreases by around 45% after 50 cycles whereas this decrease is 75% for normal LT-$LiCoO_2$.

In conclusion, it has been shown that lithium-containing nanostructured materials may be prepared by a hard templating route, by first forming the transition-metal oxide and then treating this with a lithium source, with preservation of the nanostructure. Both one-dimensional nanowire LT-$LiCoO_2$ (based on SBA-15) and three-dimensional mesoporous LT-$LiCoO_2$ (based on KIT-6) have been synthesized with highly crystalline structures. Preliminary electrochemical data demonstrate that the nanostructured materials exhibit superior capacity retention on cycling compared with normal LT-$LiCoO_2$.

Experimental Section

The preparation of the mesoporous silicas, SBA-15 and KIT-6, has been described previously.[7,10,13] A typical synthesis of nanostructured LT-$LiCoO_2$ was as follows: $Co(NO_3)_2 \cdot 6H_2O$ (98%, Aldrich; 1 g) was dissolved in ethanol (20 mL) then mesoporous silica (2 g) was added. After stirring at room temperature until all the solution had been absorbed, the sample was heated slowly to 300 °C and calcined at that temperature for 3 h. The impregnation procedure was repeated, and the sample was then calcined at 500 °C for 3 h. The resulting sample

 © 2005 Wiley-VCH Verlag GmbH & Co. KGaA, Weinheim

was treated twice with a 10% solution of HF in water to remove the silica template, then washed with water and ethanol several times, and then dried at 60°C. 0.2 g of the as-prepared nanostructured Co_3O_4 was mixed with excess $LiOH{\cdot}H_2O$ (0.6 g) in ethanol (20 mL). The solvent was removed by stirring overnight at room temperature, and the mixture was calcined at 400°C for 1 h. The final product was washed with water and ethanol several times to remove the unreacted lithium salt and then dried at 60°C for 2 h. The materials were characterized by TEM (Jeol JEM-2011), PXRD (Stoe STADI/P diffractometer operating in transmission mode with $Fe_{K\alpha_1}$ radiation, $\lambda = 1.936$ Å), low-angle XRD (Rigaku/MSC, D/max-rB with $Cu_{K\alpha 1}$ radiation, $\lambda = 1.541$ Å), and N_2 adsorption (Hiden IGA porosimeter).

Electrochemical cells were constructed by mixing the active material, Kynar 2801 (a copolymer based on polyvinylidene fluoride), and Super P carbon in the weight ratio 80:10:10. The mixture was cast onto Al foil from THF using a Doctor–Blade technique. After evaporation of the solvent at 45°C, the electrodes were assembled into cells with a Li electrode and LP 30 electrolyte (Merck; 1M $LiPF_6$ in 1:1 v/v EC:DMC, EC = ethylene carbonate, DMC = dimethyl carbonate). The cells were constructed and handled in an Ar-filled MBraun glovebox. Electrochemical measurements were carried out using a Biologic MacPile II system.

Received: May 13, 2005
Published online: September 13, 2005

Keywords: intercalations · lithium · mesoporous materials · template synthesis · transition metals

[1] a) M. Antonietti, G. A. Ozin, *Chem. Eur. J.* **2004**, *10*, 29; b) J. T. Hu, T. W. Odom, C. M. Lieber, *Acc. Chem. Res.* **1999**, *32*, 435; c) C. N. R. Rao, M. Nath, *Dalton Trans.* **2003**, 1; d) M. Remskar, *Adv. Mater.* **2004**, *16*, 1497; e) F. Schuth, *Angew. Chem.* **2003**, *115*, 3730; *Angew. Chem. Int. Ed.* **2003**, *42*, 3604; f) R. Tenne, *Angew. Chem.* **2003**, *115*, 5280; *Angew. Chem. Int. Ed.* **2003**, *42*, 5124.

[2] a) A. Taguchi, F. Schuth, *Microporous Mesoporous Mater.* **2005**, *77*, 1; b) C. C. Wang, J. Y. Ying, *Chem. Mater.* **1999**, *11*, 3113; c) D. M. Antonelli, *Adv. Mater.* **1999**, *11*, 487.

[3] F. Jiao, P. G. Bruce, *Angew. Chem.* **2004**, *116*, 6084; *Angew. Chem. Int. Ed.* **2004**, *43*, 5958.

[4] A. S. Aricò, P. G. Bruce, B. Scrosati, J.-M. Tarascon, W. van Schalkwijk, *Nat. Mater.* **2005**, *4*, 366.

[5] a) D. M. Antonelli, J. Y. Ying, *Angew. Chem.* **1995**, *107*, 2202; *Angew. Chem. Int. Ed. Engl.* **1995**, *34*, 2014; b) Z. R. Tian, W. Tong, J. Y. Wang, N. G. Duan, V. V. Krishnan, S. L. Suib, *Science* **1997**, *276*, 926; c) P. D. Yang, D. Y. Zhao, D. I. Margolese, B. F. Chmelka, G. D. Stucky, *Nature* **1998**, *396*, 152.

[6] a) H. F. Yang, D. Y. Zhao, *J. Mater. Chem.* **2005**, *15*, 1217; b) J. Lee, S. Han, T. Hyeon, *J. Mater. Chem.* **2004**, *14*, 478.

[7] F. Kleitz, S. H. Choi, R. Ryoo, *Chem. Commun.* **2003**, 2136.

[8] a) S. C. Laha, R. Ryoo, *Chem. Commun.* **2003**, 2138; b) B. Z. Tian, X. Y. Liu, H. F. Yang, S. H. Xie, C. Z. Yu, B. Tu, D. Y. Zhao, *Adv. Mater.* **2003**, *15*, 1370; c) E. L. Crepaldi, G. Soler-Illia, D. Grosso, F. Cagnol, F. Ribot, C. Sanchez, *J. Am. Chem. Soc.* **2003**, *125*, 9770; d) F. Jiao, B. Yue, K. K. Zhu, D. Y. Zhao, H. Y. He, *Chem. Lett.* **2003**, *32*, 770; e) W. C. Li, A. H. Lu, C. Weidenthaler, F. Schuth, *Chem. Mater.* **2004**, *16*, 5676; f) V. Escax, M. Imperor-Clerc, D. Bazin, A. Davidson, *C. R. Chim.* **2005**, *8*, 663.

[9] K. K. Zhu, B. Yue, W. Z. Zhou, H. Y. He, *Chem. Commun.* **2003**, 98.

[10] B. Z. Tian, X. Y. Liu, L. A. Solovyov, Z. Liu, H. F. Yang, Z. D. Zhang, S. H. Xie, F. Q. Zhang, B. Tu, C. Z. Yu, O. Terasaki, D. Y. Zhao, *J. Am. Chem. Soc.* **2004**, *126*, 865.

[11] Y. Q. Wang, C. M. Yang, W. Schmidt, B. Spliethoff, E. Bill, F. Schuth, *Adv. Mater.* **2005**, *17*, 53.

[12] Y. K. Zhou, C. M. Shen, H. L. Li, *Solid State Ionics* **2002**, *146*, 81.

[13] D. Y. Zhao, J. L. Feng, Q. S. Huo, N. Melosh, G. H. Fredrickson, B. F. Chmelka, G. D. Stucky, *Science* **1998**, *279*, 548.

[14] a) K. Mizushima, P. C. Jones, P. J. Wiseman, J. B. Goodenough, *Mater. Res. Bull.* **1980**, *15*, 783; b) L. A. Depicciotto, M. M. Thackeray, W. I. F. David, P. G. Bruce, J. B. Goodenough, *Mater. Res. Bull.* **1984**, *19*, 1497; c) R. J. Gummow, M. M. Thackeray, W. I. F. David, S. Hull, *Mater. Res. Bull.* **1992**, *27*, 327; d) R. J. Gummow, D. C. Liles, M. M. Thackeray, *Mater. Res. Bull.* **1993**, *28*, 235.

[15] Y. Shao-Horn, S. A. Hackney, A. J. Kahaian, M. M. Thackeray, *J. Solid State Chem.* **2002**, *168*, 60.

 © 2005 Wiley-VCH Verlag GmbH & Co. KGaA, Weinheim